Progress of Theoretical Physics, Vol. 50, No. 4, October 1973

Thermoelectric Power of Copper

Jiro YAMASHITA and Setsuro ASANO

Institute for Solid State Physics, University of Tokyo
Roppongi, Minatoku, Tokyo 106

(Received April 16, 1973)

The thermoelectric power of copper at high temperature is calculated by a realistic model. The Fermi vector, Fermi velocity and wave functions are determined by APW. The phonon spectrum is calculated by the Born-von Karman atomic-force-constant model. The matrix elements of the electron-phonon interaction are given by the single site approximation. It is found that the calculated value of the thermoelectric power has a positive sign and its magnitude is roughly equal to the observed one.

§ 1. Introduction

The positive value of the thermoelectric power (TEP) of noble metals has been a subject of a lively discussion in recent years.[1)~8)] It seems to us, however, that a correct answer was already guessed,[9),10)] or was already given,[8)] though semiquantitatively. The remaining task is to evaluate it from the first principle and to see whether the result is in good agreement with experiment. This task is not easy, however, even when the problem is limited to evaluation of TEP at high temperature. For a complete answer, it is required to have a detailed knowledge of the electronic states on the Fermi surface and of the perturbation potential by which the electrons are scattered. The former problem will be solved by the band calculation and the answer will be almost unique, but it is difficult to determine the latter with a full confidence. Rather, we must rely on a model with a limited validity. Therefore, if a calculation of TEP depends critically upon the model of the electron-phonon interaction (E-PH), then we shall be at a loss. As will be mentioned later, however, the real situation at copper is not so bad. If some plausible models of E-PH are adopted, the calculated value of TEP of copper by each model is found to be rather insensitive to the model. It will be concluded in the present paper that the theoretical value of TEP of copper has a positive sign and its magnitude is roughly equal to the observed one.

§ 2. Method of calculation

We shall follow the method of calculation developed in the paper of Hasegawa and Kasuya,[8)] which will be referred to as HK. The electrical conductivity will be given by (HK(12))

$$\sigma = (e^2/12\pi^3\hbar) \int \tau_k v_k dS_k = (e^2/12\pi^3\hbar) S\langle l \rangle, \tag{1}$$

where S is the area of the Fermi surface, v_k and τ_k are the velocity and the relaxation time of each Bloch state on the Fermi surface with the wave vector $\boldsymbol{k}$ and $\langle l \rangle$ is the mean free path defined by (1). In the following, integration over the Fermi surface is always replaced by summation over 30×48 points on the Fermi surface. Then, $\langle l \rangle$ is

$$\langle l \rangle = (\delta S/S) \sum_i \tau_i v_i = (\delta S/S) \sum_i l_i, \tag{2}$$

where $S = 30 \times 48\ \delta S$ and l_i is the mean free path at the point i. Hasegawa and Kasuya solved the Boltzmann equation by Taylor's method[2] with the vector mean free path $\boldsymbol{\Lambda}(\boldsymbol{k})$ defined by $\tau_k = (\boldsymbol{v_k} \cdot \boldsymbol{\Lambda}(\boldsymbol{k}))/v_k^2$. (See HK (7)$\sim$(10).) The transition matrix between the initial state $\boldsymbol{k}$ and the final state $\boldsymbol{k}'$ on the Fermi surface is given by (HK (6))

$$Q(\boldsymbol{k}', \boldsymbol{k}) = (\hbar/4\pi^2 MNk_B T) \sum_\xi |M_{q\xi}(\boldsymbol{k}', \boldsymbol{k})|^2 n_{q\xi}(n_{q\xi}+1), \tag{3}$$

where $\boldsymbol{q}$ is the wave vector of phonons in the first Brillouin zone:

$$\boldsymbol{q} = \boldsymbol{k}' - \boldsymbol{k} + \boldsymbol{G}_n. \tag{4}$$

Here, M is the ion mass, N is the number of ions in the unit volume, k_B is the Boltzmann constant, T is the absolute temperature and G_n is one of the reciprocal lattice vectors. Following HK we shall calculate σ by Taylor's method. A more conventional method is also usable to calculate the relaxation time. As is well known, it gives

$$1/\tau_k = \int \{(\boldsymbol{v}_{k'} - \boldsymbol{v}_k)^2/2v_k v_{k'}\} Q(\boldsymbol{k}', \boldsymbol{k}) dS_{k'}/\hbar v_{k'}. \tag{5}$$

As a matter of convenience, we shall use the reduced velocity $\langle \boldsymbol{v}_k \rangle$ instead of $\boldsymbol{v}_k$, which is defined by $\langle \boldsymbol{v}_k \rangle = \boldsymbol{v}_k/v_F$, then we see easily that $\langle l \rangle$ or σ is proportional to v_F^2. Here, v_F is the mean velocity on the Fermi surface. Then, let us introduce L_i by $L_i = l_i/v_F^2$, and then

$$\langle l \rangle = (\delta S/S) v_F^2 \sum_i L_i. \tag{6}$$

As for the matrix element $M_{q\xi}(\boldsymbol{k}', \boldsymbol{k})$, HK chose a phenomenological way (HK (3)), but we shall proceed along another line. First, let us introduce the so-called "single site approximation", although it may be an oversimplified model. The matrix element in this approximation may be written as

$$M_{q\xi}(\boldsymbol{k}', \boldsymbol{k}) = (\psi_{k'}(\boldsymbol{r}) | \boldsymbol{e}(\boldsymbol{q}\xi) \cdot \nabla V(r) | \psi_k(\boldsymbol{r})), \tag{7}$$

where $\psi_k(\boldsymbol{r})$ and $\psi_{k'}(\boldsymbol{r})$ are the Bloch function of the initial and the final state, respectively, $\boldsymbol{e}(\boldsymbol{q}, \xi)$ is the polarization vector of phonon and $V(r)$ is the self-consistent muffin-tin potential which is used to calculate the band energy $E(\boldsymbol{k})$

and the wave function $\psi_{\boldsymbol{k}}(\boldsymbol{r})$ by KKR or APW method. The constant potential outside the inscribed sphere will be denoted by V_0. Following Mott and Jones we may transform the matrix element as a function of the logarithmic derivative of the radial wave function $R_l(r_i; E_F)$, or of the phase shift $\eta_l(E_F)$. Here, E_F is the Fermi energy and r_i is the radius of the inscribed sphere. The APW wave function is defined as follows:

$$\psi_{\boldsymbol{k}}(r) = \sum \alpha_n(\boldsymbol{k}) \exp(i\boldsymbol{k}_n \boldsymbol{r}) \qquad \text{in outer region,}$$

$$\psi_{\boldsymbol{k}}(r) = \sum a_\nu(\boldsymbol{k}) R_l(r; E_F) C_\nu(\theta, \varphi) \qquad \text{in the inscribed sphere,}$$

where $\boldsymbol{k}_n = \boldsymbol{k} + \boldsymbol{G}_n$, $C_\nu(\theta, \varphi)$ is the normalized cubic harmonics. The index ν specifies the angular part of the wave function in the following order: $(1, y, z, x, xy, yz, z^2-(1/2)(x^2+y^2), xz, x^2-y^2, y^3-(3/5)y, xyz, y(z^2-x^2), z^3-(3/5)z, x(y^2-z^2), z(x^2-y^2), x^3-(3/5)x$ and so on.) For convenience $R_l(r; E_F)$ is normalized in the inscribed sphere and the total charge is normalized to one per electron in the Wigner-Seitz cell. Then, the coefficients $\alpha_n(\boldsymbol{k})$ are normalized so as to give the amount of charge outside the inscribed sphere, and $a_\nu(\boldsymbol{k})$ are normalized so as to give the amount of charge in the inscribed sphere. The derivation of the matrix element $M_{\boldsymbol{q}\xi}(\boldsymbol{k}', \boldsymbol{k})$ was already given in several papers,[11)~14)] so that we shall show only a part of them as an illustration:

$$M_{\boldsymbol{q}\xi}(\boldsymbol{k}', \boldsymbol{k}) = e_x(\boldsymbol{q}\xi) M_x + e_y(\boldsymbol{q}\xi) M_y + e_z(\boldsymbol{q}\xi) M_z. \tag{8}$$

In order to express M_i in a compact form, let us introduce a notation

$$a(i, j) = a_i(\boldsymbol{k}) a_j(\boldsymbol{k}') - a_j(\boldsymbol{k}) a_i(\boldsymbol{k}'). \tag{9}$$

Then M_z is written as

$$\begin{aligned} M_z = &-A_{sp}(1/\sqrt{3}) a(1, 3) - A_{pd}\{(2/\sqrt{15}) a(3, 7) + (1/\sqrt{5}) a(2, 6) \\ &+ (1/\sqrt{5}) a(4, 8)\} - A_{df}\{(1/\sqrt{7})(a(5, 11) + a(8, 14) + a(9, 15)) \\ &+ (3/\sqrt{35}) a(7, 13) - (\sqrt{3/35})(a(6, 10) + a(8, 16))\}. \end{aligned} \tag{10}$$

The electron-phonon coupling constants $A_{l, l+1}$ are defined as follows:

$$A_{l, l+1} = (\tan \eta_l - \tan \eta_{l+1}) R_l(r_i; E_F) R_{l+1}(r_i; E_F) / B(l, l+1), \tag{11}$$

where

$$B(l, l+1) = (j_l(\kappa r_i) - \tan \eta_l n_l(\kappa r_i))(j_{l+1}(\kappa r_i) - \tan \eta_{l+1} n_{l+1}(\kappa r_i)) \tag{12}$$

and $\kappa = (E_F - V_0)^{1/2}$. This matrix element of E-PH does not converge to the expected value of $-(2/3)E_F$ at $q=0$, in the sense of the pseudopotential theory. In order to hold this condition it might be better to add the perturbation potential $V(-Qe^2/r)$ outside the inscribed sphere. Then the matrix element M_z is modified to MAT_z defined by

$$MAT_z = M_z + S_z,$$

where S_z is given by (in rydberg unit)

$$S_z=-\sum_n\sum_m \alpha_m(\boldsymbol{k}')\alpha_n(\boldsymbol{k})K_{nm,z}(8\pi Q/K_{nm}^2)\sin(K_{nm}r_i)/K_{nm}r_i\varepsilon(K_{nm}). \quad (13)$$

Here $K_{nm}=|\boldsymbol{k}_{m'}-\boldsymbol{k}_n|$ and $\varepsilon(x)$ is the usual dielectric function of free electron gas modified only by the effective mass m^*. There are two ways to hold the condition at $q=0$ mentioned before. One is to take $Q=1$ but m^* is adjusted and the other is to take $m^*=1$ but Q is adjusted.

In the following we shall denote the single site approximation as Model I and the modified one as Model II. As will be shown later, there is no large difference between these two. The model proposed by Lee and Nowak (Model LN)[15),16)] has the same form of the matrix element as Model I, but the values of the coupling constants A are widely different from ours. For the purpose of illustration, the two sets of values of tan η_l, Nowak's and ours, are shown in Table I. Our values are obtained from the real crystal potential and a characteristic feature is the large value of the d-phase shift, while Nowak used a kind of pseudopotential and the d-phase shift is quite small, but the s- and p-phase shift are much larger. In Table II the two sets of values of A are also shown. Since the Model LN is quite different from ours, we want to introduce some models between them, in which the constants A_{pd} and A_{df} are not much different from the previous ones, but the value of A_{sp} may be much different. These phenomenological models will be denoted by Models III and IV.

Table I. Phase shifts of copper at the Fermi energy.

	Nowak	present paper
tan η_0	0.898	−0.0818
tan η_1	0.238	0.0854
tan η_2	−0.025	−0.132
tan η_3		−0.0003

Table II. The value of the coupling constants of electron-phonon interaction in various models.

	Model I	Model II	Model III	Model IV	Model LN
A_{sp}	0.14	0.14	−0.15	−0.20	−0.565
A_{pd}	−0.30	−0.30	−0.35	−0.35	−0.366
A_{df}	2.4	2.4	2.0	2.0	0.45
m^*	—	0.815	1.0	1.0	—
Q	—	1.0	1.5	1.5	—

The phonon spectrum is calculated by the Born-von Karman atomic-force-constant model. The force constants are those given by Nicklow et al.[17)]

The band structure of copper is determined by KKR with the $X\alpha$ potential. The value of α is taken as 2/3. This self-consistent potential is capable to well reproduce the observed shape of the Fermi surface, but the potential is slightly modified to be l-dependent so as to reproduce the observed shape of the Fermi surface with sufficient accuracy. In practice, the Fermi vectors are determined

by Halse's formula.[18] For calculation of the electrical conductivity, 30 points are selected on the 1/48 of the Fermi sarface. The band energy and the wave functions of these states are calculated by APW. They have the same energy E_F in the practical sense. The Fermi velocity is determined both by Halse's formula and by the band calculation at the same 30 points as before. The values of the Fermi velocity obtained by Halse's formula are smaller than those by the band calculation, because the correction due to the electron-phonon interaction is included in the former. The average value of the ratio v_k (band)$/v_k$ (Halse) at 30 points is evaluated as 1.08. The same kind of the argument has been made by Nowark and Lee[19] and their corresponding value is 1.10. The band velocity will be used in the present paper. The area of the Fermi surface is also evaluated by the aid of Halse's formula. The electrical conductivity is evaluated from the mean free path at 30 points. It is also evaluated from 6 points suitably selected on the 1/48 of the Fermi surface. It is possible to make the value of the conductivity from 6 points only 0.96 times of that from the 30 points. The six k vectors, their band velocity, the enhancement factor due to E-PH and the character of the wave functions are shown in Table III. It is remarkable that the amount of charge outside the inscribed sphere is much smaller than that expected from the free electron picture. Further, the d-components of the wave function have a considerable amplitude on the Fermi surface, and even the f-components are important through the contribution from the d-f scattering to resistivity.

Table III. The six $\boldsymbol{k}$ vectors on the Fermi surface, their velocity, their enhancement factor due to E-PH, the components of wave functions. The notations s, p, d, f and out mean the amount of charge of s, p, d and f character in the inscribed sphere and the amount of charge outside the inscribed sphere, respectively.

No.	k_x	k_y	k_z	v_{band}/v_{free}	$(1+\lambda)$	s	p	d	f	out
1	0.60586	0.42287	0.32894	0.716	1.134	0.0592	0.3866	0.3354	0.0050	0.2138
2	0.59710	0.44128	0.21518	0.774	1.076	0.1212	0.2636	0.4478	0.0028	0.1646
3	0.67239	0.30090	0.21340	0.819	1.066	0.1422	0.2467	0.4550	0.0020	0.1541
4	0.59843	0.44226	0.08303	0.751	1.034	0.1625	0.1838	0.5193	0.0014	0.1330
5	0.68952	0.30774	0.08426	0.804	1.041	0.1652	0.2155	0.4762	0.0018	0.1413
6	0.77360	0.15933	0.07449	0.864	1.116	0.1668	0.3116	0.3415	0.0064	0.1737

§ 3. Results

(A) *resistivity*

Resistivity is calculated by Taylor's method. The mean free path is also calculated from (5). Both methods give almost the same value of the resistivity. The difference is at most 5% and such difference is insignificant in the present paper. The results on resistivity are shown in Table IV. The numerical values

Table IV. Resistivity of copper calculated by various models and its experimental value.

T	Model I	Model II	Model III	Model IV	Model LN	experiment
295	1.45	1.78	1.68	1.68	1.36	1.70
50	0.077	0.091	0.066	0.060	0.043	0.050
ratio	19	20	25	28	32	34

Table V. Anisotropy in the relaxation time at the six points on the Fermi surface in various models. The left is the values at 295K and the right is the value at 50K. The unit is 10^{-14} sec.

No.	Model II		Model III		Model IV		Model LN	
1	2.08	30.0	2.49	47.4	2.58	52.9	3.67	105.6
2	2.96	55.5	3.09	76.9	3.10	81.4	4.00	122.8
3	3.09	58.8	3.18	81.5	3.17	86.4	3.95	128.2
4	3.84	89.3	3.65	104	3.59	106	4.29	139.3
5	3.52	73.8	3.47	94.3	3.43	97.6	4.04	131.0
6	2.49	43.6	2.82	68.0	2.83	73.2	3.30	102.2

Table VI. The thermoelectric power. Here ξ is defined in (14) and th is the third term in (15). The experimental value of ξ at room temperature is -1.6.

T	Model I		Model II		Model III		Model IV		Model LN	
	th	ξ	th	ξ	th	ξ	th	ξ	th	ξ
290	−2.2	−1.6	−2.5	−1.9	−1.8	−1.2	−1.7	−1.1	−1.9	−1.3
50	—	—	−3.3	−2.7	−2.7	−2.1	—	—	—	—

of the relaxation time at six points mentioned before are also shown in Table V. As seen from Table IV, the agreement between theory and experiment is good in all cases at room temperature, but the temperature dependence of resistivity is slightly different by the models. As for the temperature dependence, Model LN seems to be the best. The difference comes from the x-dependence of resistivity. Here, x denotes the difference in the wave vectors divided by $2k_F$.

$$x=|\boldsymbol{k}'-\boldsymbol{k}|/2k_F.$$

It is instructive to analyse the total resistivity to each component coming from the different region of x. The formula (5) is used for the purpose and Δx, the width of a fraction, is taken as 0.025. A smooth curve is drawn from the original histogram. They are shown in Figs. 1, 2, 3 and 4 corresponding to Models II, III, IV and LN. The characteristic feature of Fig. 1 is a large and sharp peak near $x=1$, which means that the effective scattering by E-PH is dominant only near $x=1$. Only the states in the neck region and near the Δ-axis are able to make a transition with the largest value of $x(x>1)$ because of the limitation of the shape of the Fermi surface. In Models I and II the relaxation time is

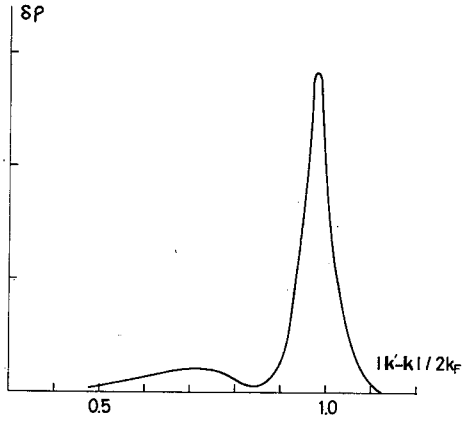

Fig. 1. Resistivity due to the transition with $|\boldsymbol{k}'-\boldsymbol{k}|/2k_F$ in Model II (relative scale). The curve is drawn from the original histogram.

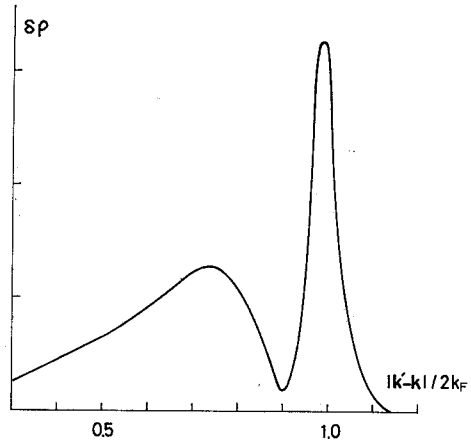

Fig. 2. The same as Fig. 1 in Model III.

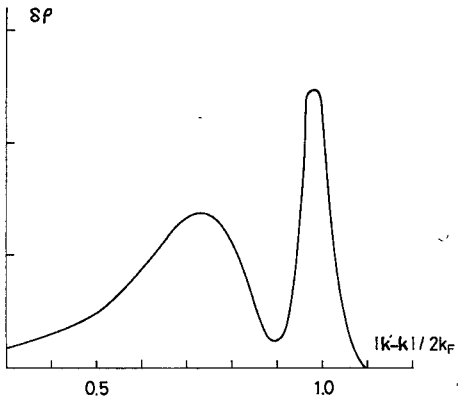

Fig. 3. The same as Fig. 1 in Model IV.

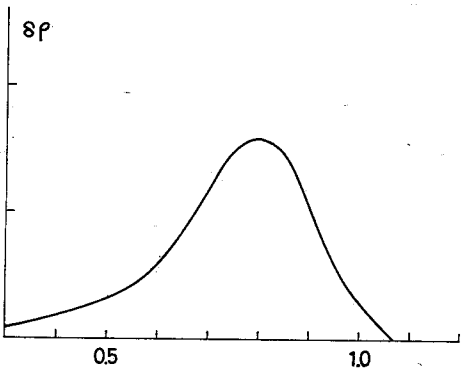

Fig. 4. The same as Fig. 1 in Model LN.

quite short in the neck region and near the Δ-axis as compared with that in other region. Moreover, in such transitions of large x, phonons of a rather small wave vector will participate, so that such transitions do not decay out easily at low temperature. This is the reason why Models I and II fail to give a correct temperature dependence at low temperature. The character of Fig. 4 is quite different. The large peak near $x=1$ disappears, but a broad peak appears around $x=0.8$. This looks like similar to the character in alkali metals, K, Rb and Cs.[10] The anisotropy of the relaxation time is also much reduced in Model LN, because the large angle scattering is much reduced as compared with Models I and II.

The high probability of the large angle scattering is the result of the dominant p-d and d-f scattering because of the large d-phase shift on the Fermi surface of Cu. The pseudopotential theory of both Harrison[20] and Moriarty[21] also give the similar prediction. Roughly speaking, the Fermi surface of Cu is

a sphere of the radius k_F, so that the difference in the initial and the final k-value in the backward scattering is close to $2k_F$. In the case of many transition metals which have very complicated Fermi surfaces, the backward scattering does not always mean the large variation in the absolute value of k.

(B) *thermoelectric power*

The diffusion term in the thermoelectric power is given by

$$Q = -(\pi^2/3)(k_B^2 T/|e|E_{free})(E_{free}\cdot\partial \log \sigma(E)/\partial E)_{E_F}$$
$$= -(\pi^2/3)(k_B^2 T/|e|E_{free})\xi, \qquad (14)$$

where E_{free} is the Fermi energy of the free electron gas whose density is equal to that of the conduction electrons in copper. The evaluation of ξ is carried out in the following way. The six points mentioned before are selected and the $\boldsymbol{k}$ vector is extended to its normal direction and the six vectors are newly determined whose energy is $E_F+\Delta E$ ($\Delta E=0.027$ Ryd). Then, the wave functions at these $\boldsymbol{k}$ points are determined again by APW. The electron velocity is calculated at the 30 points mentioned before on the 1/48 of the energy surface of $E_F+\Delta E$ by APW. In order to evaluate the quantity $(1/S)(\Delta S/\Delta E)$ or $S+\Delta S$, where S is the area of the Fermi surface and $S+\Delta S$ is the area of the surface of $E_F+\Delta E$, we choose 550 points on the 1/48 of Halse's Fermi surface and construct the new surface of $E_F+\Delta E$ ($\Delta E=0.01$ Ryd) by extending each $\boldsymbol{k}_F$ vector to its normal direction by $\Delta k=\Delta E/2v_F(\boldsymbol{k})$. Here $v_F(\boldsymbol{k})$ denotes the Halse Fermi velocity. Then the area $S+\Delta S$ is determined by a numerical integration.

It is convenient to divide ξ into three parts:

$$\xi = E_{free}\cdot\{(1/S)(\Delta S/\Delta E) + (2/v_F)(\Delta v/\Delta E)$$
$$+ (1/\sum_i L_i)(\Delta \sum_i L_i/\Delta E)\}_{E_F}. \qquad (15)$$

As for the first and second terms in (15) Ziman has evaluated the value of $E_{free}\cdot[(1/S)(\Delta S/\Delta E)_{E_F}+(1/v_F)(\Delta v/\Delta E)_{E_F}]$ by the eight cone model as 0.45,[1] while it is 1.5 in the free electron model. The large reduction of the positive factor in ξ has a decisive meaning to get a correct value of ξ of copper. In our calculation the value of the first term in (15) is 0.2 and that of the second term is 0.4, so that our value is slightly smaller than Ziman's. In fact, it is not easy to evaluate $(\Delta S/\Delta E)$ with sufficient accuracy, because the large part of the gain in ΔS throughout the belly region is compensated by the loss of the area in the neck region. The accuracy of the value $(\Delta v/\Delta E)$ is also limited, because an accurate evaluation of the second derivative of the energy on the Fermi surface is required. The value of this factor is also negative at the neck region and positive at the belly, so that it results in a large compensation as a whole. It is, however, quite certain that the values of the first and the second term in (15) are much smaller than the corresponding value in the free electron model. The value of the third term in (15) depends upon the model and also temperature.

The calculation is carried out by the method mentioned previously and the results are shown in Table VI, while the observed value at room temperature is -1.6. As seen from the Table, the agreement between theory and experiment is reasonable irrespective of the models. We may say that according to theory the thermoelectric power of copper at high temperature has a positive sign and has a magnitude roughly equal to the observed one. As mensioned previously, the reason why the value of ξ is negative at copper was well anticipated by Ziman and Robinson and Dow and especially by Hasegawa and Kasuya. The reason is the increase in the rate of large angle scattering with increase of an electron energy near the Fermi surface. As an example, let us consider the case of Model LN, where about 37% of the resistance comes from the large angle scattering with $x>0.8$. When the energy surface is raised by 0.027 Ryd, then the third term in (15) is evaluated as -1.9. If the contribution is divided into two parts, that is, from $x<0.8$ and $x>0.8$, then the former is of 0.6 and the latter is of -2.5. The corresponding values in Model III are 0.2 and -2.0, respectively. The increase in resistivity with increase of electron energy comes from two factors. One is the change in the length of the k vector and the other is the change in the wave functions. In order to see the former contribution, we make an artificial calculation with increased $\boldsymbol{k}$ vectors and original wave functions. The value of ξ becomes -0.8 instead of -1.9 in Model II.

The value of ξ changes with temperature in the low temperature region ($T<100$°K) where the resistivity deviates much from a linear law of T, because the shape of the curve shown in Figs. 1$\sim$4 changes considerably with temperature. As seen from Table IV, the amount of change is not small, so that it is not safe to ascribe the deviation from a linear law in TEP at low temperature only to the phonon-drag effect, although the latter contribution seems to be larger than the former. It must be noted here that the correction term in TEP discussed by Tsuji[6] and Bross and Hacker[7] was not considered in the present paper.

(C) *the mass shift*

Here the thermal band mass is denoted by m_{th} and the observed thermal mass is denoted by m^*_{th}. Then the mass shift due to E-PH is defined by

$$m^*_{\text{th}} = (1+\lambda)\, m_{\text{th}}. \tag{16}$$

The value of λ is evaluated as 0.12 at Model II by the formula (19) in HK. The Models I, III and IV are not usable for the purpose, because the condition at $q=0$ mentioned before is not satisfied by these models. Nowak[16] has calculated λ at Model LN by essentially the same method as ours and obtained the value 0.12.

§ 4. Discussion

The single site approximation seems to be usable for noble metals as the first approximation, but it is clearly an oversimplified model. It emphasizes the

large angle scattering too much. The effective perturbation may extend beyond the single site, and there may be a correction term which enhances the small angle scattering as illustrated in Figs. 2 and 3. The pseudopotential approach of LN may be better than the single site approximation, although the underlying physical picture is not quite clear for us. It must be noted that the good result is obtained, only when the true wave functions are used for the matrix element of EP. The magnitude of A_{pd} of Model LN is nearly equal to ours, and the main contribution to resistivity comes from the p-d scattering in both cases, but the origin is quite different. It is the large p-phase shift in Model LN, while it is the large d-phase shift in our models. (Since the d-phase shift is quite small, there is no trace of the d-bands near the Fermi surface in Model LN.) At present, Model LN and a model like the modified single site approximation as Model III or IV are recommendable. We do not know which one of them is closer to the real situation.

References

1) J. M. Ziman, Adv. in Phys. **10** (1961), 1.
2) P. L. Taylor, Proc. Roy. Soc. **A275** (1963), 200, 209.
3) F. J. Blatt, Phys. Rev. **99** (1955), 1735.
4) R. Barrie, Phys. Rev. **103** (1956), 1581.
5) H. Jones, Proc. Phys. Soc. **A68** (1958), 1191.
6) M. Tsuji, J. Phys. Soc. Japan **13** (1958), 133.
7) H. Bross and W. Hacker, Z. Naturforsch. **16a** (1961), 632.
8) A. Hasegawa and T. Kasuya, J. Phys. Soc. Japan **25** (1968), 141.
9) J. M. Ziman, *The Physics of Metals*, edited by J. M. Ziman (Cambridge University Press, 1969), p. 278.
10) J. E. Robinson and J. D. Dow, Phys. Rev. **171** (1968), 815.
11) D. C. Golibersuch, Phys. Rev. **157** (1967), 532.
12) K. Sinha, Phys. Rev. **169** (1968), 477.
13) M. J. G. Lee and V. Heine, Phys. Rev. **B5** (1972), 3839.
14) P. B. Allen and M. J. G. Lee, Phys. Rev. **B5** (1972), 3848.
15) M. J. G. Lee, Phys. Rev. **B2** (1970), 250.
16) D. Nowak, Phys. Rev. **B6** (1972), 3691.
17) R. M. Nicklow, G. Gilat, H. G. Smith, L. J. Raubenheimer and M. K. Wilkinson, Phys. Rev. **164** (1967), 922.
18) M. R. Halse, Phil. Trans. Roy. Soc. London **265** (1969), 507.
19) D. Nowak and M. J. G. Lee, Phys. Rev. **B5** (1972), 2851.
20) W. A Harrison, Phys. Rev. **181** (1969), 1036.
21) J. A. Moriarty, Phys. Rev. **B1** (1970), 1363.